

Local self-interaction correction method with a simple scaling factor

Selim Romero,^{1,2} Yoh Yamamoto,¹ Tunna Baruah,^{1,2} and Rajendra R. Zope^{1,2, a)}

¹⁾*Department of Physics, University of Texas at El Paso, El Paso, Texas 79968, USA*

²⁾*Computational Science Program, University of Texas at El Paso, El Paso, Texas 79968, USA*

(Dated: 20 October 2020)

A recently proposed local self-interaction correction (LSIC) method [Zope *et al.* J. Chem. Phys., 2019,**151**, 214108] when applied to the simplest local density approximation provides significant improvement over standard Perdew-Zunger SIC (PZSIC) for both equilibrium properties such as total or atomization energies as well as properties involving stretched bond such as barrier heights. The method uses an iso-orbital indicator to identify the single-electron regions. To demonstrate the LSIC method, Zope *et al.* used the ratio z_σ of von Weizsäcker τ_σ^W and total kinetic energy densities τ_σ , ($z_\sigma = \tau_\sigma^W / \tau_\sigma$) as a scaling factor to scale the self-interaction correction. The present work further explores the LSIC method using a simpler scaling factor as a ratio of orbital and spin densities in place of the ratio of kinetic energy densities. We compute a wide array of both, equilibrium and non-equilibrium properties using the LSIC and orbital scaling methods using this simple scaling factor and compare them with previously reported results. Our study shows that the present results with simple scaling factor are comparable to those obtained by LSIC(z_σ) for most properties but have slightly larger errors. We furthermore study the binding energies of small water clusters using both the scaling factors. Our results show that LSIC with z_σ has limitation in predicting the binding energies of weakly bonded system due to the inability of z_σ to distinguish weakly bonded region from slowly varying density region. LSIC when used with density ratio as a scaling factor, on the other hand, provides good description of water cluster binding energies, thus highlighting the appropriate choice of iso-orbital indicator.

^{a)}Electronic mail: rzope@utep.edu

I. INTRODUCTION

Kohn-Sham (KS) formulation of density functional theory (DFT)¹⁻³ is widely used to study electronic structures of atoms, molecules, and solids because of its low computational cost and availability of easy to use software packages. The practical application of DFT requires an approximation to the exchange-correlation (XC) functional. The simplest form of the XC functional is the local spin density approximation (LSDA)^{1,4} which belongs to the lowest rung of ladder of the XC functionals⁵. The higher rungs of the ladder contains more complex and more accurate functionals- generalized gradient approximation (GGA), meta-GGA, hybrid, and functionals that include the virtual orbitals. Practically all efforts in the functional design have been focused on improving the energetics or equilibrium properties such as atomization energies, bond distances, etc. The majority of the density functional approximations suffer from self-interaction errors (SIE) though the magnitude of error can vary from one class of functionals to another or from one parameterization to another in a given class of functional. The SIE occurs as a result of incomplete cancellation of self-Coulomb energy by the self-exchange energy of the approximate XC functional.

Many failures of density functional approximations (DFAs) have been attributed to the SIE. The SIE causes the potential to decay asymptotically as $-exp(-r)$ instead of the correct $-1/r$ decay for finite neutral systems. As a result the DFAs produce errors such as too shallow eigenvalues of valence orbitals, inaccurate chemical reaction barriers, electron delocalization errors, incorrect charges on dissociated fragments, incorrect binding energies for anions, etc.^{4,6-8} The $-1/r$ asymptotic behavior is also important for the computation of electronic properties that are sensitive to virtual orbitals and long-range density such as excited states for example.

A number of approaches to remove the SIEs have been proposed.⁹⁻¹⁹ Early approaches^{9,10} used orbitalwise schemes to eliminate the SIE but used functionals related to Slater's $X\alpha$ method²⁰. The most widely used approach to remove SIE is the one proposed by Perdew and Zunger (PZ)⁴. Their approach is commonly referred to as PZ self-interaction correction (PZSIC) where the one-electron SIE due to both exchange and correlation are removed from a DFA calculation on an orbital by orbital basis. PZSIC provides the exact cancellation for one- and two-electron self-interaction (SI), but not necessarily for many-electron SI²¹. It has been applied to study properties of atoms, molecules, clusters, and solids.^{8,12,15,16,22-70}

The PZSIC is an orbital dependent theory and when used with the KS orbitals results in size-extensivity problem. In PZSIC, local orbitals are used to keep the corrections size-extensive. Traditionally, PZSIC requires solving the so called Pederson or localization equations (LE)^{71,72} to find the set of local orbitals that minimizes the total energy. Solving the LE and finding the optimal orbitals compliant with the condition is computationally expensive since it requires solving the LE for each pair of orbitals. Pederson *et al.* in 2014 used Fermi-Löwdin orbitals^{73,74} (FLOs) to solve the PZSIC equations. This approach is known as FLO-SIC^{75,76}. FLOs are Löwdin orthogonalized set of Fermi orbitals (FOs) that can be obtained from the KS orbitals. The FOs depend on the density matrix and spin density. The FLOs are the local orbitals that make PZSIC total energy unitarily invariant. For construction of FLOs, Fermi orbital descriptor (FOD) positions are used as $3N$ parameters in space that can be optimized in analogous manner to the optimization of atomic positions in molecular structure optimization. FLOSIC method has computational advantage over traditional PZSIC since it requires optimizing only $3N$ parameters instead of N^2 parameters for the transformation to the local orbitals.

Earlier applications of FLO-SIC with LSDA showed significant improvements in atomic and molecular properties over SI-uncorrected LSDA performance^{46,66,77,78}. Naturally, FLOSIC was later also applied to more sophisticated XC functionals than LSDA, such as Perdew–Burke–Ernzerhof (PBE) and Strongly Constrained and Appropriately Normed (SCAN), to see whether SIC improves the performance of those functionals in the higher rungs^{17,47,60–63,65,67–70,79–83}. PZSIC when applied to semi-local functional such as PBE GGA and SCAN meta-GGA provides good descriptions in stretched bond situation and provides bound atomic anions but this improvement occurs at the expense of worsening^{32,80,81,84–86} the performance for properties where SI-uncorrected DFA performs well. Shahi *et al.*⁸⁰ recently attributed the poor performance of PZSIC with GGAs and higher rung functionals to the nodality of the local orbital densities. The use of complex localized orbitals with nodeless densities in PZSIC calculations by Klüpfel, Klüpfel and Jónsson⁸⁵ show that the complex orbital densities alleviate the worsening of atomization energies when used with PBE functional. This conflicting performance of PZSIC is called the paradox of SIC by Perdew and coworkers⁸⁷. The worsening of energetics pertaining to equilibrium region primarily is a result of the overcorrecting tendency of PZSIC. A few methods have been proposed to mitigate the overcorrecting tendency of PZSIC by scaling down the SIC contribution. Jónsson’s group simply scaled the

SIC by a constant scaling factor⁸⁴. In a similar spirit, Vydrov *et al.* proposed a method to scale down the SIC according to an orbital dependent scaling factor (OSIC)³⁴. This method however does not provide significant improvement over all properties. It improved over PZSIC atomization energies but worsened barrier heights. Moreover, the scaling approach by Vydrov *et al.* results in worsening the asymptotic description of the effective potential causing atomic anions to be unbound. Ruzsinszky *et al.*⁸⁸ found that many-electron SIE and fractional-charge dissociation behavior of positively charged dimers reappear in the OSIC of Vydrov *et al.*. A new selective OSIC method, called SOSIC, by Yamamoto and coworkers⁸³ that selectively scales down the SIC in many electron regions overcomes the deficiencies of the OSIC method and gives stable atomic anions as well as improved total atomic energies. It also improves the barrier heights over the OSIC method. Very recently, Zope *et al.*¹⁷ proposed a new SIC method which identifies the single-electron region using iso-orbital indicators and corrects for SIE in a pointwise fashion by scaling down the SIC. The iso-orbital indicator serves as a weight in numerical integration and identifies both the single-orbital regions where full correction is needed and the uniform density regions where the DFAs are already exact and correction is not needed. They called the new SIC method local-SIC (LSIC)¹⁷ and assessed its performance for a wide array of properties using LSDA. Unlike the PZSIC, the LSIC provided remarkable performance for both equilibrium properties like atomization energies and stretched bond situations that occur in barrier height calculation.

The LSIC method makes use of iso-orbital indicator to identify one-electron region. It offers additional degree of freedom in that suitable iso-orbital can be used or designed to identify one-electron region or tune the SIC contribution in a pointwise manner. In the original LSIC work, Zope *et al.* used a ratio of von Weiszäcker and total kinetic energy densities as a choice for the local scaling factor. This iso-orbital indicator has been used in construction of self-correlation free meta-GGAs, in the regional SIC¹⁵ and also in local hybrid functionals^{89,90}. Several different choices for the local scaling factors are already available in literature. Alternatively, new iso-orbital indicators particularly suitable for LSIC can be constructed. In this work, we explore the performance of the LSIC method using a simple ratio of the orbital density and spin density as weight of SIC correction at a given point in space. This is the same scaling factor used by Slater to average the Hartree-Fock exchange potential in his classic work that introduced Hartree-Fock-Slater method²⁰. We

refer to this choice of scaling factor as $\text{LSIC}(w)$ for the remainder of this manuscript and use $\text{LSIC}(z)$ to refer to the first LSIC application where the scaling factor is the ratio of von Weizsäcker kinetic energy and kinetic energy densities. We investigate the performance of $\text{LSIC}(w)$ for a few atomic properties: total energy, ionization potentials, and electron affinities. For molecules, we calculated the total energies, atomization energies, and the dissociation energies of a few selected systems. We find that $\text{LSIC}(w)$ provides comparable results to $\text{LSIC}(z)$. We also show a case where $\text{LSIC}(w)$ performs better than the original $\text{LSIC}(z)$. Additionally, we examine the performance of the scaling factor w based on the density ratio with the OSIC scheme.

In the following section, brief descriptions of the PZSIC, OSIC, and LSIC methods are presented. These methods are implemented using the FLOs. Therefore, very brief definitions pertaining to FLOs are also presented. The results and discussion are presented in the next sections.

II. THEORY AND COMPUTATIONAL METHOD

A. Perdew-Zunger and Fermi-Lowdin Self-Interaction Correction

In the PZSIC method⁴, SIE is removed on an orbital by orbital basis from the DFA energy as

$$E^{PZSIC-DFA} = E^{DFA}[\rho_{\uparrow}, \rho_{\downarrow}] - \sum_{i\sigma}^{occ} \{U[\rho_{i\sigma}] + E_{XC}^{DFA}[\rho_{i\sigma}, 0]\}, \quad (1)$$

where i is the orbital index, σ is the spin index, ρ ($\rho_{i\sigma}$) is the electron density (local orbital density), $U[\rho_{i\sigma}]$ is the exact self-Coulomb energy, and $E_{XC}^{DFA}[\rho_{i\sigma}, 0]$ is the self-exchange-correlation energy for a given DFA XC functional. Perdew and Zunger applied this scheme to atoms using the Kohn-Sham orbitals. For larger systems the Kohn-Sham orbitals can be delocalized which would result in the violation of size extensivity. Therefore local orbitals are required. This was recognized long ago by Slater and Wood⁹¹ in 1971 and was also emphasized by Gopinathan¹⁰ in the context of self-interaction-correction of Hartree-Slater method and later by Perdew and Zunger in the context of approximate Kohn-Sham calculations. Subsequent PZSIC calculations by Wisconsin group^{71,72,92,93} used local orbitals in variational implementation. It was shown by Pederson and coworkers that local orbitals used in the Eq. (1) must satisfy the localization equations (LE) for variational minimization

of energy. The LE for the orbitals $\phi_{i\sigma}$ is a pairwise condition and is given as

$$\langle \phi_{i\sigma} | V_{i\sigma}^{SIC} - V_{j\sigma}^{SIC} | \phi_{j\sigma} \rangle = 0. \quad (2)$$

In the FLOSIC approach, FLOs are used in stead of directly solving the Eq. (2). First, FOs ϕ^{FO} are constructed with the density matrix and spin density at special positions in space called Fermi orbital descriptor (FOD) positions as

$$\phi_i^{FO}(\vec{r}) = \frac{\sum_j^{N_{occ}} \psi_j(\vec{a}_i) \psi_j(\vec{r})}{\sqrt{\rho_i(\vec{a}_i)}}. \quad (3)$$

Here, i and j are the orbital indexes, and ψ is the KS orbital, ρ_i is the electron spin density, and \vec{a}_i is the FOD position. The FOs are then orthogonalized with the Löwdin's scheme to form the FLOs. The FLOs are used for the calculation of the SIC energy and potential. In this method, the optimal set of FLOs are found by finding the FODs that minimizes total energy. This optimization process is similar to that for geometry optimization. We note that FLOs can be used in all three SIC (PZSIC, OSIC, and LSIC) methods.

B. Orbitalwise scaling of SIC

As mentioned in Sec. I, PZSIC tends to overcorrect the DFA energies and several modifications to PZSIC were proposed to *scale down* the PZSIC correction. In the OSIC method of Vydrov *et al*³⁴ mentioned in Introduction Eq. (1) is modified to

$$E^{OSIC-DFA} = E_{XC}^{DFA}[\rho_{\uparrow}, \rho_{\downarrow}] - \sum_{i\sigma}^{occ} X_{i\sigma}^k (U[\rho_{i\sigma}] + E_{XC}^{DFA}[\rho_{i\sigma}, 0]), \quad (4)$$

where each local orbitalwise scaling factor $X_{i\sigma}^k$ is defined as

$$X_{i\sigma}^k = \int z_{\sigma}^k(\vec{r}) \rho_{i\sigma}(\vec{r}) d^3\vec{r}. \quad (5)$$

Here, i indicates the orbital index, σ is the spin index, z_{σ} is the iso-orbital indicator, and k is an integer. The quantity z_{σ} is used to interpolate the single-electron regions ($z_{\sigma} = 1$) and uniform density region ($z_{\sigma} = 0$). In their original work, Vydrov *et al.* used $z_{\sigma} = \tau_{\sigma}^W / \tau_{\sigma}$ to study the performance of OSIC with various XC functionals where $\tau_{\sigma}^W(\vec{r}) = |\vec{\nabla} \rho_{\sigma}(\vec{r})|^2 / (8\rho_{\sigma}(\vec{r}))$ is the von Weiszäcker kinetic energy density and $\tau_{\sigma}(\vec{r}) = \frac{1}{2} \sum_i |\vec{\nabla} \psi_{i\sigma}(\vec{r})|^2$ is the non-interacting kinetic energy density. Satisfying the gradient expansion in ρ requires

$k \geq 1$ for LSDA, $k \geq 2$ for GGAs, and $k \geq 3$ for meta-GGA. Vydrov *et al.*, however, used various values of k to study its effect on the OSIC performance.

In their subsequent work, Vydrov *et al.*¹⁶ used

$$w_{i\sigma}^k(\vec{r}) = \left(\frac{\rho_{i\sigma}(\vec{r})}{\rho_{\sigma}(\vec{r})} \right)^k, \quad (6)$$

the weight used by Slater in averaging Hartree-Fock potential, as a scaling factor instead of kinetic energy ratio. They repeated the OSIC calculations using $w_{i\sigma}$ in place of z_{σ} in Eq. (5). Notice that Eq. (6) contains a local orbital index, this weight is thus an orbital dependent quantity. $w_{i\sigma}$ approaches unity at single orbital regions since $\rho_{\sigma}(\vec{r}) = \rho_{i\sigma}(\vec{r})$ at this limit. Similarly, $w_{i\sigma}$ approaches zero at many-electron region since $\rho_{\sigma}(\vec{r}) \gg \rho_{i\sigma}(\vec{r})$ at this condition. It was reported that the OSIC with Eq. (6) showed comparable performance as $z_{\sigma} = \tau_{\sigma}^W / \tau_{\sigma}$ despite of its simpler form.

C. LSIC

Though OSIC had some success in improving the performance with SIC, the approach leads to parameter k dependent performance. Also, it gives $-X_{HO}/r$ asymptotic potential instead of $-1/r$ for finite neutral systems and it results in inaccurate description of dissociation behavior²¹. In addition, many-electron SIE and fractional-charge dissociation behavior of positively charged dimers reemerge with the OSIC⁸⁸. The recent LSIC method by Zope *et al.* applies the SIC in a different way than OSIC and retains desirable beneficial features of PZSIC. In LSIC, the SIC energy density is scaled down *locally* as follows,

$$E_{XC}^{LSIC-DFA} = E_{XC}^{DFA}[\rho_{\uparrow}, \rho_{\downarrow}] - \sum_{i\sigma}^{occ} (U^{LSIC}[\rho_{i\sigma}] + E_{XC}^{LSIC}[\rho_{i\sigma}, 0]), \quad (7)$$

where

$$U^{LSIC}[\rho_{i\sigma}] = \frac{1}{2} \int d^3\vec{r} z_{\sigma}(\vec{r})^k \rho_{i\sigma}(\vec{r}) \int d^3\vec{r}' \frac{\rho_{i\sigma}(\vec{r}')}{|\vec{r} - \vec{r}'|}, \quad (8)$$

$$E_{XC}^{LSIC}[\rho_{i\sigma}, 0] = \int d^3\vec{r} z_{\sigma}(\vec{r})^k \rho_{i\sigma}(\vec{r}) \epsilon_{XC}^{DFA}([\rho_{i\sigma}, 0], \vec{r}). \quad (9)$$

LSIC uses an iso-orbital indicator to apply SIC pointwise in space. An ideal choice of iso-orbital indicator should be such that LSIC reduces to DFA in uniform gas limit and reduces to PZSIC in the pure one-electron limit. To demonstrate the LSIC concept Zope *et al.* used $z_{\sigma} = \tau_{\sigma}^W / \tau_{\sigma}$ as an iso-orbital indicator. In this study, however, we use $w_{i\sigma}(\vec{r}) = \rho_{i\sigma}(\vec{r}) / \rho_{\sigma}(\vec{r})$

in place for z_σ in Eqs. (8) and (9). We refer to the LSIC with $z_\sigma(\vec{r})$ as LSIC(z) and LSIC with $w_{i\sigma}(\vec{r})$ as LSIC(w) to differentiate the two cases.

D. Computational details

All of the calculations were performed using the developmental version of FLOSIC code^{78,94}, a software based on the UTEP-NRLMOL code. PZSIC, OSIC, and LSIC methods using FLOs are implemented in this code. FLOSIC/NRLMOL code uses Gaussian type orbitals⁹⁵ whose default basis sets are in similar quality as quadruple zeta basis sets. We used the NRLMOL default basis sets throughout our calculations. For calculations of atomic anions, long range s, p, and d single Gaussian orbitals are added to give a better description of the extended nature of anions. The exponents β of these added single Gaussians were obtained using the relation, $\beta(N + 1) = \beta(N)^2/\beta(N - 1)$, where N is the N -th exponent. FLOSIC code uses a variational integration mesh⁹⁶ that provides accurate numerical integration.

In this work, our focus is on the LSDA functional because LSIC applied to LSDA is free from the gauge problem⁹⁷ unlike GGAs and meta-GGAs where a gauge transformation is needed since their XC potentials are not in the Hartree gauge. We used an SCF energy convergence criteria of 10^{-6} Ha for the total energy and an FOD force tolerance of 10^{-3} Ha/bohr for FOD optimizations in FLOSIC calculations. For OSIC and LSIC calculations, we used respective FLOSIC densities and FODs as a starting point and performed a non-self-consistent calculation of energy on the FLOSIC densities. Several values for the scaling power k are used in the LSIC(w) and OSIC(w) calculations. The additional computational cost of the scaling factor in OSIC and LSIC is very small compared to a regular FLO-PZSIC calculation.

III. RESULTS AND DISCUSSION

The LSIC method was assessed for a wide array of electronic structure properties to obtain a good understanding of how the new methodology performs. Here, we assess the performance of LSIC(w) vis-a-vis LSIC(z) and OSIC(w) using the same array of electronic properties. We considered total energies, ionization potentials, and electron affinities for atoms and

atomization energies, reaction barrier heights, and dissociation energies for molecules.

A. Atoms

In this section, we present our results on total energies, ionization potentials, and electron affinities for atoms.

1. Total energy of atoms

We compared the total atomic energies of the atoms $Z = 1 - 18$ against accurate non-relativistic values reported by Chakravorty *et al.*⁹⁸. Various integer values of k were used for LSIC(w) and OSIC(w). The differences between our calculated total energies with $k = 1$ and the reference values are plotted in Fig. 1. The plot clearly shows the effect of scaling on the total energies of atoms. Consistent with reported results, the LSDA total energies are too high compared to accurate reference values⁹⁸ whereas PZSIC consistently underestimates the total energies due to its over correcting tendency. The LSIC method, where both scaling factors performs similarly, provides the total energies closer to the reference values than LSDA and PZSIC-LSDA. Likewise, OSIC method also reduces the overcorrection bringing the total energies to close agreement with the reference values. The mean absolute errors (MAEs) in total energy with respect to the reference for various k values are shown in Table I. The MAE of PZSIC is 0.381 Ha whereas LSIC(w) and OSIC(w) show MAEs of 0.061 and 0.074 Ha, respectively, with $k = 1$. LSIC(z) shows a better performance than OSIC(w) and LSIC(w). The LSIC(w) MAE is in the same order of magnitude as the earlier reported MAE of LSIC(z) of 0.041 Ha¹⁷. As the value of k increases, the magnitude of SI-correction is reduced. This result in MAEs become larger for $k > 1$ eventually approaching the LSDA numbers.

For $k = 0$ the scaled methods correctly produce the PZSIC results. The scaling is optimal for $k = 1$ which results in optimal magnitude of SI-correction for LSIC(w) and almost right magnitude for OSIC(w). The magnitude of SIC energy of each orbitals when compared among different methods, it is found that the SIC correction in LSIC(w) is larger (i.e. less scaling down) for the core orbitals than in the LSIC(z). This trend is reversed for the valence orbitals (cf. Table II). It can be seen from Table II that total SIC energy in both

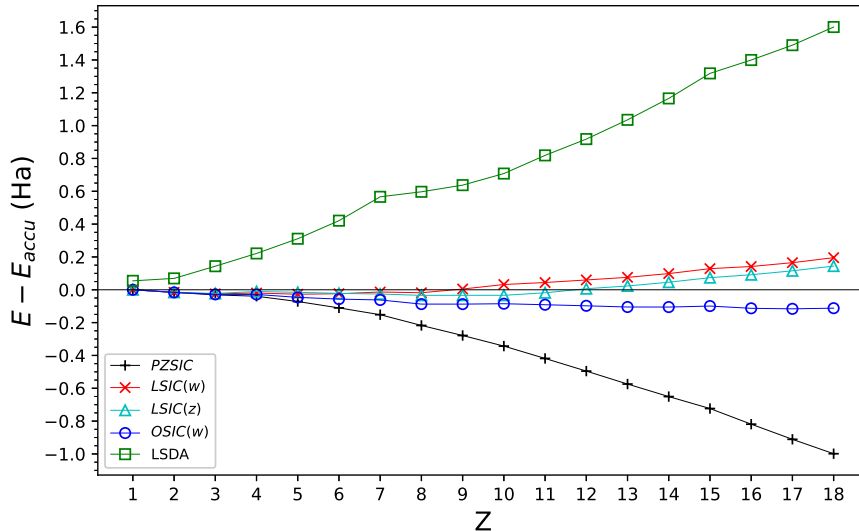


FIG. 1: Total energy difference (in hartree) of atoms $Z = 1 - 18$ with respect to accurate nonrelativistic estimates⁹⁸.

methods is essentially similar in magnitude. However the way scaling factors behave affects the orbitalwise contribution to the total SIC energy. This changes the SIC potentials and results in two methods performing differently for cations and anions. For OSIC(w), we find the smallest MAE for $k = 2$ of 0.070 Ha, a value slightly smaller than that for $k = 1$.

2. Ionization potential

The ionization potential (IP) is the energy required to remove an electron from the outermost orbital. Since electron removal energy is related to the asymptotic shape of the potential, one can expect SIC plays an important role in determining IPs. We calculated the IPs using the Δ SCF method defined as

$$E_{IP} = E_{cat} - E_{neut} \quad (10)$$

where E_{cat} is the total energy in the cationic state and E_{neut} is the total energy at the neutral state. The calculations were performed for atoms from helium to krypton, and we compared the computed IPs against the experimental ionization energies⁹⁹. FODs were relaxed both for neutral atoms and for their cations. Fig. 2 shows the difference of calculated IPs with respect to the reference values. MAEs with different methods are shown in Table III for

TABLE I: Mean absolute error of the total atomic energy (in hartree) for atoms $Z = 1 - 18$ with respect to accurate nonrelativistic estimates⁹⁸.

Method	MAE
PZSIC	0.381
LSIC($z, k = 1$)	0.041
LSIC($w, k = 1$)	0.061
LSIC($w, k = 2$)	0.196
LSIC($w, k = 3$)	0.277
LSIC($w, k = 4$)	0.332
OSIC($w, k = 1$)	0.074
OSIC($w, k = 2$)	0.070
OSIC($w, k = 3$)	0.135

TABLE II: Magnitude of SIC energy (in hartree) per orbital type in Ar atom for each method.

Orbital	PZSIC	LSIC(z)	LSIC(w)	OSIC(w)
1s	-0.741	-0.387	-0.490	-0.584
2sp ³	-0.126	-0.070	-0.050	-0.062
3sp ³	-0.016	-0.017	-0.006	-0.008
Total SIC	-2.616	-1.473	-1.421	-1.729

a subset $Z = 2 - 18$ as well as for the entire set $Z = 2 - 36$ to facilitate a comparison against literature. For the smaller subset, $Z = 2 - 18$, the MAEs are 0.248 and 0.206 eV for PZSIC and LSIC(z), respectively. The MAE for OSIC($w, k = 1$) is 0.223 eV showing an improvement over PZSIC. LSIC($w, k = 1$) shows MAE of 0.251 eV, a comparable error with PZSIC. MAEs increase for LSIC($w, k \geq 2$) and OSIC($w, k \geq 2$) in comparison to their respective $k = 1$ MAEs. Interestingly, however, when we considered the entire set of atoms ($Z = 2 - 36$), LSIC(w) has MAEs of 0.238 and 0.216 eV for $k = 1$ and $k = 2$ respectively showing smaller errors than PZSIC (MAE, 0.364 eV) but LSIC(w) falls short of LSIC(z)

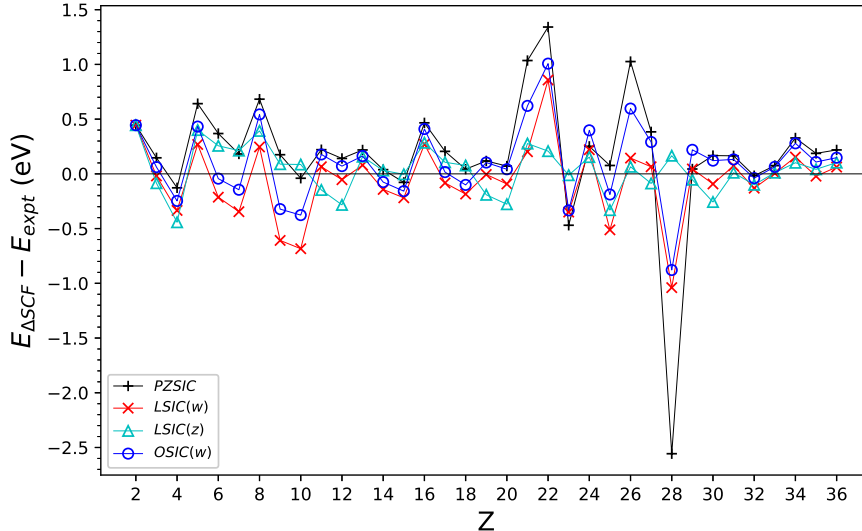


FIG. 2: Energy difference in ionization potential (in eV) for a set of atoms $Z = 2 - 36$ with respect to experimental values⁹⁹.

which has the smallest error (MAE, 0.170 eV). For this case, OSIC(w , $k = 1 - 3$) shows better performance than PZSIC but not as well as LSIC(w) for a given k . LSIC(z) performs better than both LSIC(w) and OSIC(w). The difference in performance between LSIC(z) and LSIC(w) implies that scaling of SIC for the cationic states is more sensitive to the choice of local scaling factor than for the neutral atoms.

3. *Electron affinity*

The electron affinity (EA) is the energy released when an electron is added to the system. We studied EAs for 20 atoms that are experimentally found to bind an electron¹⁰⁰. They are H, Li, B, C, O, F, Na, Al, Si, P, S, Cl, K, Ti, Cu, Ga, Ge, As, Se, and Br atoms. The EAs were calculated using the Δ SCF method $E_{EA} = E_{neut} - E_{anion}$ and values were compared against the experimental EAs¹⁰⁰.

Fig. 3 shows deviation of EA from reference experimental values for various methods. The MAEs are summarized in Table IV. We have presented the MAEs in two sets, the smaller subset which contains hydrogen through chlorine (12 EAs) and for the complete set, hydrogen to bromine (20 EAs).

TABLE III: Mean absolute error of ionization potentials (in eV) for set of atoms $Z = 2 - 18$ and $Z = 2 - 36$ with respect to experiment⁹⁹.

Method	Z=2-18 (17-IPs)	Z=2-36 (35-IPs)
PZSIC	0.248	0.364
LSIC($z, k = 1$)	0.206	0.170
LSIC($w, k = 1$)	0.251	0.238
LSIC($w, k = 2$)	0.271	0.216
LSIC($w, k = 3$)	0.297	0.247
LSIC($w, k = 4$)	0.324	0.284
OSIC($w, k = 1$)	0.223	0.267
OSIC($w, k = 2$)	0.247	0.247
OSIC($w, k = 3$)	0.255	0.259

For 12 EAs, MAEs for PZSIC and LSIC(z) are 0.152 and 0.097 eV, respectively. OSIC(w) shows MAE of 0.152 eV for $k = 1$, the same performance as PZSIC. LSIC(w), however, does not perform as well as PZSIC, giving the MAEs of 0.235 eV for $k = 1$. In both case, the error decrease slightly for $k \geq 2$ but there is no significant impact on their performance.

For 20 EAs, the similar trend persists. PZSIC and LSIC(z) have MAEs of 0.190 and 0.102 eV, respectively. The MAEs of LSIC(w) are in the range 0.176 – 0.224 eV for $k = 1 - 4$ and those of OSIC(w) are between 0.155 – 0.172 eV for $k = 1 - 3$. Again, decrease in error is observed as the value in k increases. In particular, larger discrepancy between LSIC($w, k = 1$) and experiment is seen for O, F, and Ti atoms. This is due to LSIC(w) raising the anion energies more than their neutral state energies.

B. Atomization energy

To study the performance of LSIC(w) for molecules, first, we calculated the atomization energies (AEs) of 37 selected molecules. Many of these molecules are subset of the G2/97 test set¹⁰¹. The 37 molecules set includes systems from the AE6 set¹⁰², small but a good representative of the main group atomization energy (MGAE109) set¹⁰³. The AEs were

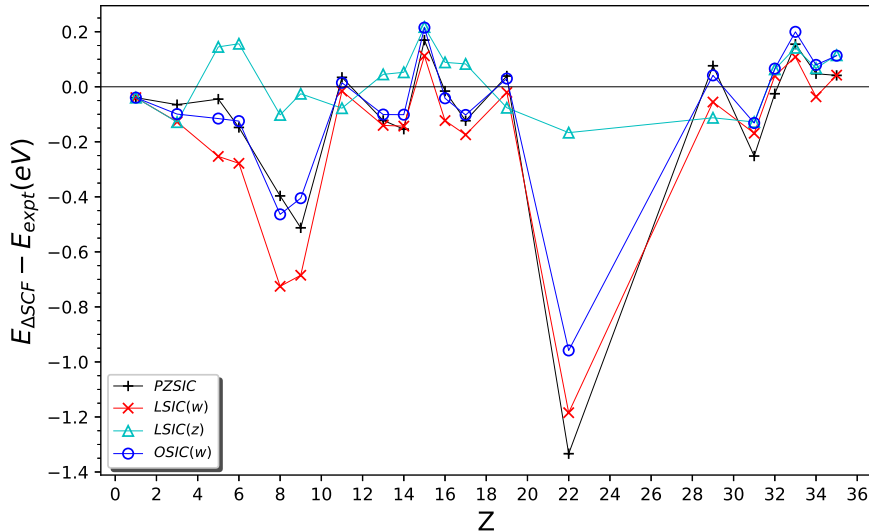


FIG. 3: Electron affinity (eV) difference for atoms $Z = 2 - 36$ with respect to experiment¹⁰⁰.

calculated by taking the energy difference of fragment atoms and the complex, that is, $AE = \sum_i^{N_{atom}} E_i - E_{mol} > 0$. E_i is the total energy of an atom, E_{mol} is the total energy of the molecule, and N_{atom} is the number of atoms in the molecule. The calculated AEs were compared to the non-spin-orbit coupling reference values¹⁰³ for AE6 set and to the experimental values¹⁰⁰ for the entire set of 37 molecules. The percentage errors obtained through various methods are shown in Fig. 4. The overestimation of AEs with PZSIC-LSDA due to overcorrection is rectified in LSIC(w). We have summarized MAEs and mean absolute percentage errors (MAPEs) of AE6 and 37 molecules from G2 set in Table V. For AE6 set, MAEs for PZSIC, LSIC(z), LSIC($w, k = 1$), and OSIC($w, k = 1$) are 57.9, 9.9, 13.8, and 33.7 kcal/mol respectively. The MAE in LSIC(z) is about 4 kcal/mol larger than LSIC($w, k = 1$) but substantially better than the PZSICs or OSIC(w). For the larger k in LSIC(w), however, the performance starts to degrade with consistent increase in the MAE of 33.5 kcal/mol for $k = 4$. This is in contrast to OSIC where the performance improves for $k = 2$ and 3 compared to $k = 1$. The scaling thus affect differently in the two methods. OSIC($w, k = 1$) tends to slightly underestimate total energies. By increasing k , total energies shift toward the LSDA total energies and improves performance for moderate increase in k . On the contrary, total energies are slightly overestimated for LSIC($w, k = 1$), and increasing k makes the energies

TABLE IV: Mean absolute error in electron affinities (in eV) for 12 EAs and 20 EAs set of atoms with respect to experiment¹⁰⁰.

Method	(12 EAs) MAE	(20 EAs) MAE
PZSIC	0.152	0.190
LSIC($z, k = 1$)	0.097	0.102
LSIC($w, k = 1$)	0.235	0.224
LSIC($w, k = 2$)	0.229	0.205
LSIC($w, k = 3$)	0.215	0.189
LSIC($w, k = 4$)	0.202	0.176
OSIC($w, k = 1$)	0.152	0.172
OSIC($w, k = 2$)	0.150	0.164
OSIC($w, k = 3$)	0.145	0.155

deviate away from the accurate estimates. OSIC($w, k = 3$) and LSIC($w, k = 1$) have a similar core orbital SIC energy. In their study of OSIC(w), Vydrov and Scuseria¹⁶ used values of k up to 5 and found the smallest error of $k = 5$ (MAE, 11.5 kcal/mol). But we expect the OSIC performance to degrade eventually for large k since increase in k results in increase in quenching of the SIC correction thus the results will eventually approach to those of DFA, in this case LSDA. For the full set of 37 molecules, PZSIC, LSIC(z), LSIC($w, k = 1$), and OSIC($w, k = 1$) show the MAPEs of 13.4, 6.9, 9.5 and 11.9%, respectively. OSIC(w) shows a slight improvement in MAPE for $k = 2$ and 3. For the larger set, LSIC(w) consistently shows smaller MAPEs than OSIC(w) for $k = 1 - 3$. All four values of k with the LSIC(w) in this study showed better performance than PZSIC for the 37 molecules set.

C. Barrier heights

Accurate description of chemical reaction barrier is challenging for DFAs since it involves calculation of energies in non-equilibrium situations. In most of the cases, the saddle point energies are underestimated since DFAs do not perform well for a non-equilibrium state that involves a stretched bond. This shortcoming of DFAs in a stretched bond case arises

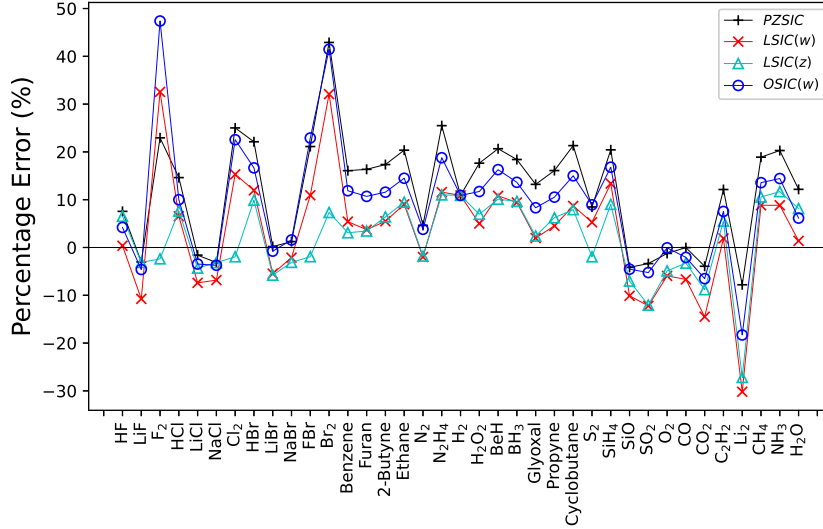


FIG. 4: Percentage errors of atomization energy (%) for a set of 37 molecules with respect to experimental values¹⁰⁰ using different scaling methods.

TABLE V: Mean absolute error (in kcal/mol) and mean absolute percentage error (in %) of atomization energy for AE6 set of molecules¹⁰³ and for the set of 37 molecules from G2 set with respect to experiment¹⁰⁰.

Method	AE6 MAE (kcal/mol)	AE6 MAPE (%)	37 molecules MAPE (%)
PZSIC	57.9	9.4	13.4
LSIC($z, k = 1$)	9.9	3.2	6.9
LSIC($w, k = 1$)	13.8	4.4	9.5
LSIC($w, k = 2$)	18.6	5.3	9.1
LSIC($w, k = 3$)	26.9	5.8	9.2
LSIC($w, k = 4$)	33.5	6.7	9.7
OSIC($w, k = 1$)	33.7	6.3	11.9
OSIC($w, k = 2$)	24.1	5.1	11.3
OSIC($w, k = 3$)	17.8	4.3	10.9

from SIE; when an electron is shared and stretched out, SIE incorrectly lowers the energy of transition state. SIC handles the stretched bond states accurately and provides a correct picture in chemical reaction paths. We studied the reaction barriers using the BH6¹⁰² set of molecules for LSIC(w) method. BH6 is a representative subset of the larger BH24¹⁰⁴ set consisting of three reactions $\text{OH} + \text{CH}_4 \rightarrow \text{CH}_3 + \text{H}_2\text{O}$, $\text{H} + \text{OH} \rightarrow \text{H}_2 + \text{O}$, and $\text{H} + \text{H}_2\text{S} \rightarrow \text{H}_2 + \text{HS}$. We calculated the total energies of left- and right-hand side and at the saddle point of these chemical reactions. The barrier heights for the forward (f) and reverse (r) reactions were obtained by taking the energy differences of their corresponding reaction states.

The mean errors (MEs) and MAEs of computed barrier heights against the reference values¹⁰² are compared in Table VI. MAEs for PZSIC, LSIC(z), LSIC($w, k = 1$), and OSIC($w, k = 1$) are 4.8, 1.3, 3.6, and 3.6 kcal/mol, respectively. PZSIC significantly improves MAE compared to LSDA (MAE, 17.6 kcal/mol), LSIC($w, k = 1$) further reduces the error from PZSIC. Its ME and MAE indicate that there is no systematic underestimation or overestimation. LSIC($w, k = 1$) also further improves the PZSIC numbers but not to the same level as LSIC(z). For $k \geq 2$, MAEs increases systematically for LSIC($w, k \geq 2$) though small MEs are seen for LSIC($w, k = 2, 3$). The performance deteriorates for $k > 2$ beyond that of PZSIC. OSIC(w) shows marginally better performance than PZSIC. Vydrov and Scuseria¹⁶ showed that the best performance is achieved with $k = 1$ (MAE, 3.5 kcal/mol). The performance improvement with OSIC is not as dramatic as LSICs in terms of MEs and MAEs where the rather large MEs are seen i Overall LSIC(w) performs better than OSIC(w) for barrier heights.

D. Dissociation and reaction energies

A pronounced manifestation of SIE is seen in dissociation of positively charged dimers X_2^+ . SIE causes the system to dissociate into two fractionally charges cations instead of X and X^+ . Here we use the SIE4x4¹⁰⁵ and SIE11¹⁰⁶ sets to study the performance of LSIC(w) and OSIC(w) in correcting the SIEs. The SIE4x4 set consists of dissociation energy calculations of four positively charged dimers at varying bond distances R from their equilibrium distance R_e such that $R/R_e = 1.0, 1.25, 1.5$ and 1.75 . The dissociation energy E_D is calculated as

$$E_D = E(X) + E(X^+) - E(X_2^+). \tag{11}$$

TABLE VI: Mean error (in kcal/mol) and mean absolute error (in kcal/mol) of BH6 sets of chemical reactions¹⁰².

Method	ME (kcal/mol)	MAE (kcal/mol)
PZSIC	-4.8	4.8
LSIC($z, k = 1$)	0.7	1.3
LSIC($w, k = 1$)	-1.0	3.6
LSIC($w, k = 2$)	-0.1	4.6
LSIC($w, k = 3$)	0.3	5.0
LSIC($w, k = 4$)	0.6	5.5
OSIC($w, k = 1$)	-3.4	3.6
OSIC($w, k = 2$)	-3.1	4.1
OSIC($w, k = 3$)	-3.0	4.6

The SIE11 set consists of eleven reaction energy calculations: five cationic reactions and six neutral reactions. These two sets are commonly used for studying the SIE related problems. The calculated dissociation and reaction energies are compared against the CCSD(T) reference values^{105,106}, and MAEs are summarized in Table VII. For the SIE4x4 set, PZSIC, LSIC(z), LSIC($w, k = 1$), and OSIC($w, k = 1$) show MAEs of 3.0, 2.6, 4.7 and 5.2 kcal/mol. LSIC(z) provides small improvement in equilibrium energies while keeping accurate behavior of PZSIC at the dissociation limit resulting in marginally better performance. LSIC(w) shows errors a few kcal/mol larger than PZSIC. This increase in error arises because LSIC(w) alters the $(\text{NH}_3)_2^+$ and $(\text{H}_2\text{O})_2^+$ dissociation curves. In LSIC(z) the scaling of SIC occurs mostly for the core orbitals (Cf. Table II) whereas LSIC(w) also includes some noticeable scaling down effect from valence orbitals. This different scaling behavior seems to contribute to different dissociation curves. Lastly, OSIC(w) has a slightly larger error than LSIC(w).

For the SIE11 set, MAEs are 11.5, 4.5, 8.3, and 11.1 kcal/mol for PZSIC, LSIC(z), LSIC($w, k = 1$), and OSIC($w, k = 1$), respectively. All scaled-down approaches we considered, LSIC(z) and LSIC(w), and OSIC(w) showed performance improvement over PZSIC. LSIC(z) shows the largest error reduction by 60%, while LSIC($w, k = 1$) shows 28% decrease in error with respect to PZSIC. OSIC(w) with $k = 1 - 3$ has slightly smaller MAEs within 1

TABLE VII: Mean absolute error for dissociation and reaction energies (in kcal/mol) of SIE4x4 and SIE11 sets of chemical reactions with respect to CCSD(T)^{105,106}.

Reaction	SIE4x4	SIE11	SIE11	
			5 cationic	6 neutral
PZSIC	3.0	11.5	14.9	8.7
LSIC(z)	2.6	4.5	2.3	6.3
LSIC(w) (k=1)	4.7	8.3	8.6	8.0
LSIC(w) (k=2)	5.5	8.3	8.3	8.3
LSIC(w) (k=3)	5.8	8.8	8.2	9.3
LSIC(w) (k=4)	5.9	9.3	8.2	10.2
OSIC(w) (k=1)	5.2	11.1	13.7	9.0
OSIC(w) (k=2)	6.0	11.0	13.5	9.0
OSIC(w) (k=3)	6.4	10.9	13.3	8.8

kcal/mol of PZSIC. LSIC(z) method improves cationic reactions more than neutral reactions with respect to PZSIC. Increase in k beyond 2 results in too much suppression of SIC and leads to increase in error for LSIC($w, k \geq 2$). LSIC(w) yielded consistently smaller MAEs than OSIC(w) but larger than LSIC(z) over the whole SIE11 reactions.

Finally, we show the ground-state dissociation curves for H_2^+ and He_2^+ in Fig. 5. As previously discussed in literature¹⁰⁷, DFAs at large separation cause the complexes to dissociate into two fragments atoms. PZSIC restores the correct dissociation behavior at the large separation distance. When LSIC is applied, the behavior of PZSIC at the dissociation limit is preserved in both LSIC(z) and present LSIC(w). For H_2^+ , a one-electron system, LSIC reproduces the identical behavior as PZSIC [Fig. 5 (a)]. For He_2^+ , a three-electron system, LSIC applies the correction to PZSIC only near equilibrium regime [Fig. 5 (b)]. LSIC brings the equilibrium energy closer to the CCSD energy compared to PZSIC energy. The implication of Fig. 5 is that the present scaling factor w performs well in differentiating the single-orbital like regions and many-electron like regions.

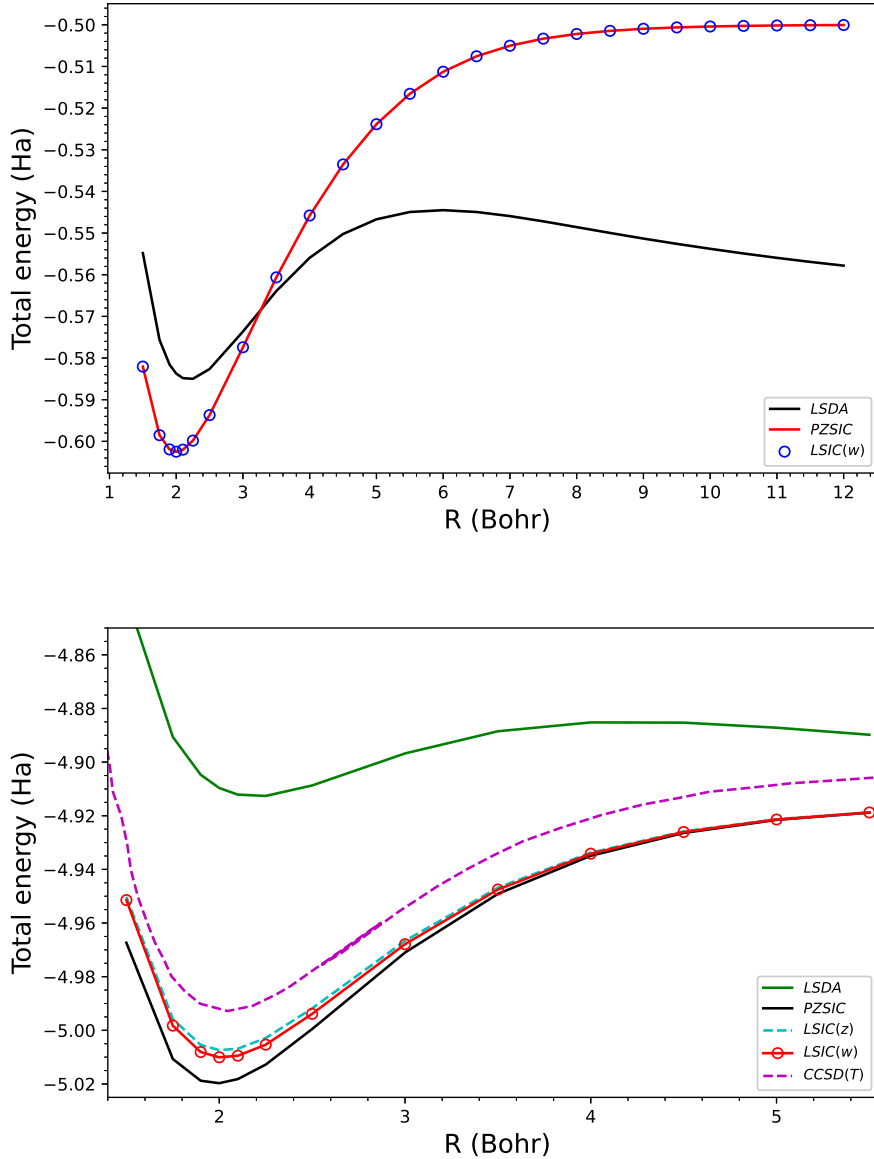


FIG. 5: Dissociation curves of (a) H_2^+ and (b) He_2^+ using various methods. The CCSD(T) curve from Ref. [21] is plotted for comparison.

E. Water binding energies: a case where LSIC(z) performs poorly

Kamal *et al.*⁷⁰ recently studied binding energies of small water clusters using the PZSIC method in conjunction with FLOs to examine the effect of SIC on binding energies of these systems. Water clusters are bonded by weaker hydrogen bonds and provide a different class of systems to test the performance of the LSIC method. Earlier studies using LSIC(z) on the

polarizabilities and ionization have shown that LSIC(z) provides an excellent descriptions of these properties when compared to the CCSD(T) results^{61,108}. Here, we study the binding energies of the water clusters. We find that the choice of iso-orbital indicator plays crucial role in water cluster binding energies. The structures considered in this work are $(\text{H}_2\text{O})_n$ ($n = 1 - 6$) whose geometries are from the WATER27 set¹⁰⁹ optimized at the B3LYP/6-311++G(2d,2p) theory. The hexamer structure has a few known isomers, and we considered the book (b), cage (c), prism (p), and ring (r) isomers. The results are compared against the CCSD(T)-F12b values from Ref. [110] in Table VIII. We obtained the MAEs of 118.9, 172.1, and 46.9 meV/H₂O for PZSIC, LSIC(z), and LSIC(w), respectively. Thus, LSIC(z) underestimates binding energies of water cluster by roughly similar magnitude as LSDA (MAE, 183.4 meV/H₂O). This is one case where LSIC(z) does not improve over PZSIC. A simple explanation for this behavior of LSIC(z) is that although z_σ used in LSIC(z) can detect the weak bond regions, it (z_σ) cannot differentiate the slow-varying density regions from weak bond regions. The $z_\sigma \rightarrow 0$ in the both situations causing the weak regions to be improperly treated. Fig. 6 (a) shows z_σ for water dimer where both slow-varying density and weak interaction regions are detected but not differentiated. As a result, the total energies of the complex shift too much in comparison to the individual water molecules. Thus, the underestimation of water cluster binding energies is due to the choice of z and not the LSIC method. Indeed by choosing the w as a scaling parameter, the binding energies are much improved. Fig. 6 (b) shows there is no discontinuity of w between the two water molecules (w_i 's of two FLOs along the hydrogen bond are plotted together in the figure). Hence unlike in LSIC(z), weak interacting region is not improperly scaled down with LSIC(w). LSIC(w) shows MAE of 46.9 meV/H₂O comparable to SCAN (MAE, 35.2 meV/H₂O). This result is interesting as SCAN uses a function that can identify weak bond interaction. So LSIC(w)-LSDA may be behaving qualitatively similar to the detection function in SCAN in weak bond regions. The study of water binding energies is so far a unique case where the original LSIC(z) performed poorly. But LSIC can be improved by simply using a different iso-orbital indicator. This case serves as a motivation in identifying appropriate iso-orbital indicator that would work for all bonding regions in LSIC.

We now provide a qualitative explanation of why LSIC(w) gives improved results over PZSIC. This reasoning is along the same line as offered by Zope *et al.*¹⁷. As mentioned in Sec. I, when the self-interaction-errors are removed using PZSIC, improved description of

TABLE VIII: The binding energy of water clusters (in meV/H₂O).

n	PZSIC	LSIC(z)	LSIC(w)	CCSD(T) ^a
2	-153.7	-34.9	-82.7	-108.6
3	-321.6	-73.9	-183.0	-228.4
4	-425.2	-125.0	-248.6	-297.0
5	-446.9	-142.7	-264.8	-311.4
6b	-467.1	-133.6	-275.0	-327.3
6c	-466.8	-113.9	-274.8	-330.5
6p	-467.7	-104.8	-276.2	-332.4
6r	-458.1	-150.5	-275.5	-320.1
MAE	118.9	172.1	46.9	

^aReference [110]

barrier heights which involve stretch bonds is obtained but the equilibrium properties like total energies, atomization energies etc. are usually deteriorated compared to the uncorrected functional. This is especially so for the functionals that go beyond the simple LSDA. Typically this is because of over correcting tendency of PZSIC. The non-empirical semilocal DFA functionals are designed to be exact in the uniform electron gas limit, this exact condition is no longer satisfied when PZSIC is applied to the functionals¹¹¹. This can be seen from the exchange energies of noble gas atoms and the extrapolation using the large- Z expansion of E_X as shown in Fig. 7. Following Ref. [111] we plot atomic exchange energies as a function of $z^{-1/3}$. Thus, the region near origin corresponds to the uniform gas limit. The plot was obtained by fitting the exchange exchange energies (E_X) of Ne, Ar, Kr, and Xe atoms (within LSIC(w)-LSDA, LSIC(z)-LSDA, and LSDA) for Ne, Ar, Kr, and Xe atoms to the curve using the following fitting function¹¹¹.

$$\frac{E_X^{approx} - E_X^{exact}}{E_X^{exact}} \times 100\% = a + bx^2 + cx^3, \quad (12)$$

where $x = Z^{-1/3}$ and a, b, and c are the fitting parameters. The LSDA is exact in the uniform gas limit. So also is LSIC(z) since the scaling factor z_σ approaches zero as the gradient of electron density vanishes while the kinetic energy density in the denominator

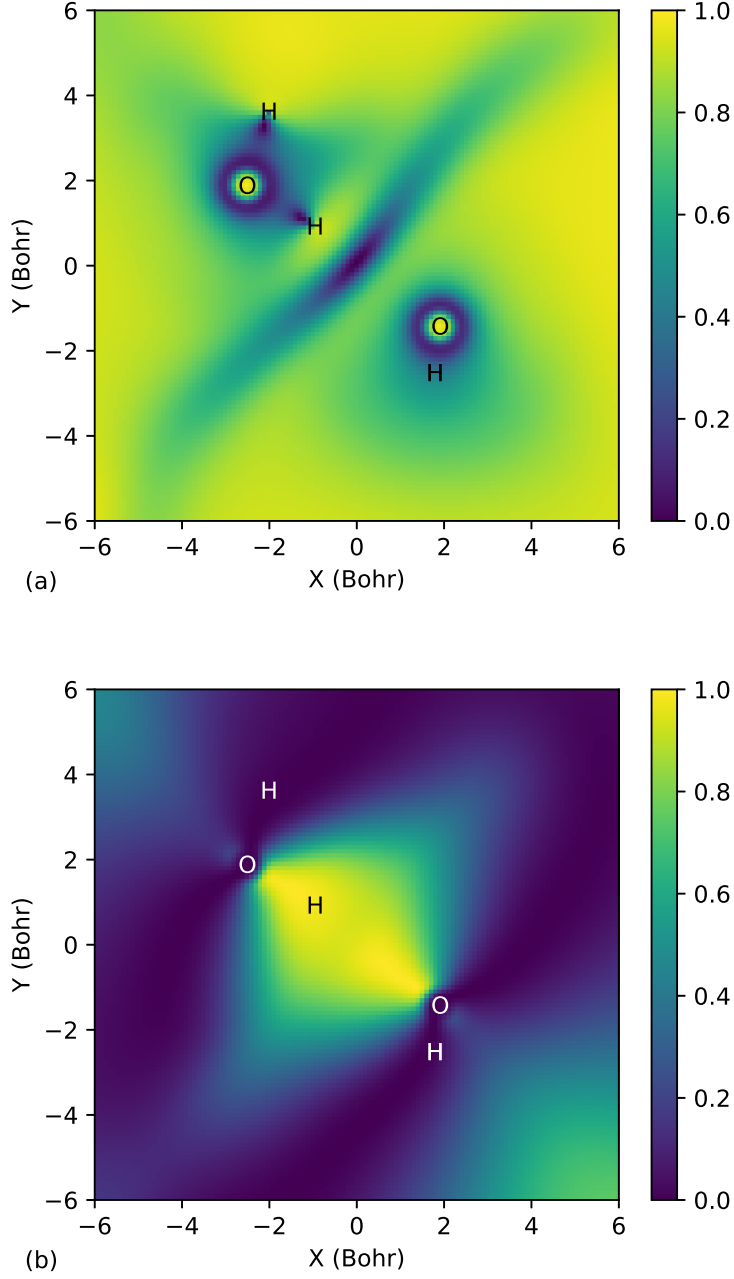


FIG. 6: Cross sectional plots of the iso-orbital indicators for water cluster dimer: (a) τ^W/τ and (b) ρ_i/ρ 's from the two FLOs along the hydrogen bond.

remains finite. The small deviation from zero seen near origin (in Fig. 7) for LSIC(z) is due to the fitting error (due to limited data point). This error is -0.62% for LSIC(z). Thus correcting LSDA using PZSIC introduces large error in the uniform gas limit. The scaling factor w used here identifies single-electron region since the density ratio approaches one

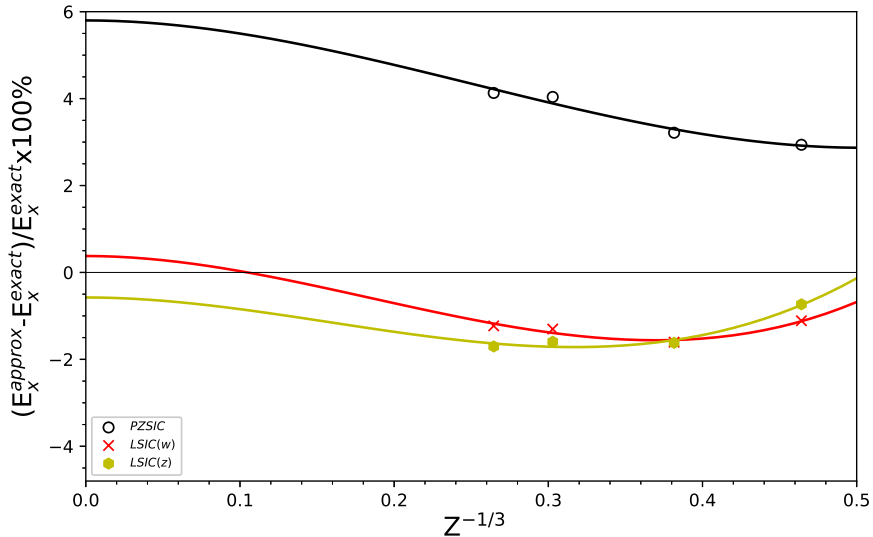


FIG. 7: Plot of percentage error of the approximated exchange energy compared to the exact exchange energy as a function of $Z^{-1/3}$.

in this limit. Fig. 7 shows that present LSIC(w) approach also recovers the lost uniform limit gas. This partly explains the success of LSIC(w). Though performance of LSIC(w) is substantially better than PZSIC-LSDA it falls short of LSIC(z). On the other hand, unlike LSIC(z) it provides good description of weak hydrogen bonds highlighting the need of identifying suitable iso-orbital indicators or scaling factor(s) to apply pointwise SIC using LSIC method. One possible choice may be scaling factor that are functions of α used in construction of SCAN meta-GGA and recently proposed¹¹² β parameter. A scaling factor containing β recently used by Yamamoto and coworkers with OSIC scheme showed improved results⁸³. Future work would involve designing suitable scaling factors involving β for use in LSIC method.

IV. CONCLUSIONS

To recapitulate, we investigated the performance of LSIC with a simple scaling factor, w , that depends only on orbital and spin densities. Performance assessment has been carried out on atomic energies, atomization energies, ionization potentials, electron affinities, barrier heights, dissociation energies etc on standard data sets of molecules. The results show that

LSIC(w) performs better than PZSIC for all properties with exception of electron affinity and a SIE4x4 subset of dissociation energies. We also compared the performance of w for LSIC against OSIC of Vydrov *et al.* Results indicate that although OSIC overall performs better than PZSIC, the improvement over PZSIC is somewhat limited. On the other hand, LSIC(w) is consistently better than OSIC(w). We have also studied the binding energies of small water clusters which are bonded by weak hydrogen bonds. Here, the LSIC(w) performs very well compared to both the PZSIC and LSIC(z) with performance comparable to SCAN. The present work shows the promise of LSIC method and also demonstrates its limitation in describing weak hydrogen bonds if used with kinetic energy ratio, z_σ as an iso-orbital indicator. This limitation is due to inability of z_σ to distinguish weak bonding regions from slowly varying density regions. The scaling factor w works differently than the scaling factor z , hence LSIC(w) provides good description of weak hydrogen bonds in water clusters. The work thus highlights importance of designing suitable iso-orbital indicator for use with LSIC that can detect weak bonding regions.

DATA AVAILABILITY STATEMENT

The data that supports the findings of this study are available within the article and the supplementary information.

CONFLICTS OF INTEREST

There are no conflicts of interest to declare.

ACKNOWLEDGEMENT

Authors acknowledge Drs. Luis Basurto, Carlos Diaz, and Po-Hao Chang for discussions and technical supports. This work was supported by the US Department of Energy, Office of Science, Office of Basic Energy Sciences, as part of the Computational Chemical Sciences Program under Award No. DE-SC0018331. Support for computational time at the Texas Advanced Computing Center through NSF Grant No. TG-DMR090071, and at NERSC is gratefully acknowledged.

REFERENCES

- ¹W. Kohn and L. Sham, *Phys. Rev.*, 1965, **140**, A1133–A1138.
- ²R. O. Jones, *Rev. Mod. Phys.*, 2015, **87**, 897.
- ³R. O. Jones and O. Gunnarsson, *Rev. Mod. Phys.*, 1989, **61**, 689–746.
- ⁴J. P. Perdew and A. Zunger, *Phys. Rev. B*, 1981, **23**, 5048–5079.
- ⁵J. P. Perdew and K. Schmidt, *AIP Conference Proceedings*, 2001, **577**, 1–20.
- ⁶E. R. Johnson, P. Mori-Sánchez, A. J. Cohen and W. Yang, *The Journal of Chemical Physics*, 2008, **129**, 204112.
- ⁷E. R. Johnson, A. Otero-de-la Roza and S. G. Dale, *The Journal of Chemical Physics*, 2013, **139**, 184116.
- ⁸J. Gräfenstein, E. Kraka and D. Cremer, *J. Chem. Phys.*, 2004, **120**, 524–539.
- ⁹I. Lindgren, *Int. J. Quantum Chem.*, 1971, **5**, 411–420.
- ¹⁰M. S. Gopinathan, *Phys. Rev. A*, 1977, **15**, 2135–2142.
- ¹¹J. P. Perdew, R. G. Parr, M. Levy and J. L. Balduz Jr, *Physical Review Letters*, 1982, **49**, 1691.
- ¹²U. Lundin and O. Eriksson, *Int. J. Quantum Chem.*, 2001, **81**, 247–252.
- ¹³P. Mori-Sánchez, A. J. Cohen and W. Yang, *The Journal of Chemical Physics*, 2006, **125**, 201102.
- ¹⁴N. I. Gidopoulos and N. N. Lathiotakis, *The Journal of Chemical Physics*, 2012, **136**, 224109.
- ¹⁵T. Tsuneda, M. Kamiya and K. Hirao, *J. Comput. Chem.*, 2003, **24**, 1592–1598.
- ¹⁶O. A. Vydrov and G. E. Scuseria, *J. Chem. Phys.*, 2006, **124**, 191101.
- ¹⁷R. R. Zope, Y. Yamamoto, C. M. Diaz, T. Baruah, J. E. Peralta, K. A. Jackson, B. Santra and J. P. Perdew, *J. Chem. Phys.*, 2019, **151**, 214108.
- ¹⁸D.-K. Seo, *Phys. Rev. B*, 2007, **76**, 033102.
- ¹⁹T. Tsuneda and K. Hirao, *The Journal of Chemical Physics*, 2014, **140**, 18A513.
- ²⁰J. C. Slater, *Physical review*, 1951, **81**, 385.
- ²¹A. Ruzsinszky, J. P. Perdew, G. I. Csonka, O. A. Vydrov and G. E. Scuseria, *J. Chem. Phys.*, 2007, **126**, 104102.
- ²²J. Garza, J. A. Nichols and D. A. Dixon, *J. Chem. Phys.*, 2000, **112**, 7880–7890.
- ²³J. Garza, R. Vargas, J. A. Nichols and D. A. Dixon, *J. Chem. Phys.*, 2001, **114**, 639–651.

- ²⁴S. Patchkovskii, J. Autschbach and T. Ziegler, *J. Chem. Phys.*, 2001, **115**, 26–42.
- ²⁵M. K. Harbola, *Solid State Commun.*, 1996, **98**, 629–632.
- ²⁶S. Patchkovskii and T. Ziegler, *J. Chem. Phys.*, 2002, **116**, 7806–7813.
- ²⁷S. Patchkovskii and T. Ziegler, *J. Phys. Chem. A*, 2002, **106**, 1088–1099.
- ²⁸S. Goedecker and C. J. Umrigar, *Phys. Rev. A*, 1997, **55**, 1765–1771.
- ²⁹V. Polo, E. Kraka and D. Cremer, *Molecular Physics*, 2002, **100**, 1771–1790.
- ³⁰V. Polo, J. Gräfenstein, E. Kraka and D. Cremer, *Theor. Chem. Acc.*, 2003, **109**, 22–35.
- ³¹J. Gräfenstein, E. Kraka and D. Cremer, *Phys. Chem. Chem. Phys.*, 2004, **6**, 1096–1112.
- ³²O. A. Vydrov and G. E. Scuseria, *J. Chem. Phys.*, 2004, **121**, 8187–8193.
- ³³O. A. Vydrov and G. E. Scuseria, *J. Chem. Phys.*, 2005, **122**, 184107.
- ³⁴O. A. Vydrov, G. E. Scuseria, J. P. Perdew, A. Ruzsinszky and G. I. Csonka, *J. Chem. Phys.*, 2006, **124**, 094108.
- ³⁵R. R. Zope, M. K. Harbola and R. K. Pathak, *The European Physical Journal D-Atomic, Molecular, Optical and Plasma Physics*, 1999, **7**, 151–155.
- ³⁶R. R. Zope, *Physical Review A*, 2000, **62**, 064501.
- ³⁷E. S. Fois, J. I. Penman and P. A. Madden, *The Journal of chemical physics*, 1993, **98**, 6352–6360.
- ³⁸J. B. Krieger, Y. Li and G. J. Iafrate, *Phys. Rev. A*, 1992, **45**, 101–126.
- ³⁹J. B. Krieger, Y. Li and G. J. Iafrate, *Phys. Rev. A*, 1992, **46**, 5453–5458.
- ⁴⁰Y. Li, J. B. Krieger and G. J. Iafrate, *Phys. Rev. A*, 1993, **47**, 165–181.
- ⁴¹S. Lehtola, M. Head-Gordon and H. Jónsson, *J. Chem. Theory Comput.*, 2016, **12**, 3195–3207.
- ⁴²G. I. Csonka and B. G. Johnson, *Theor. Chim. Acta*, 1998, **99**, 158–165.
- ⁴³L. Petit, A. Svane, M. Lüders, Z. Szotek, G. Vaitheeswaran, V. Kanchana and W. Temmerman, *J. Phys. Cond. Matter*, 2014, **26**, 274213.
- ⁴⁴S. Kümmel and L. Kronik, *Rev. Mod. Phys.*, 2008, **80**, 3.
- ⁴⁵T. Schmidt, E. Kraisler, L. Kronik and S. Kümmel, *Phys. Chem. Chem. Phys.*, 2014, **16**, 14357–14367.
- ⁴⁶D.-y. Kao, M. Pederson, T. Hahn, T. Baruah, S. Liebing and J. Kortus, *Magnetochemistry*, 2017, **3**, 31.
- ⁴⁷S. Schwalbe, T. Hahn, S. Liebing, K. Trepte and J. Kortus, *J. Comput. Chem.*, 2018, **39**, 2463–2471.

- ⁴⁸H. Jónsson, K. Tsemekhman and E. J. Bylaska, Abstracts of Papers of the American Chemical Society, 2007, pp. 120–120.
- ⁴⁹M. M. Rieger and P. Vogl, *Phys. Rev. B*, 1995, **52**, 16567.
- ⁵⁰W. Temmerman, A. Svane, Z. Szotek, H. Winter and S. Beiden, *Electronic Structure and Physical Properties of Solids*, Springer, 1999, pp. 286–312.
- ⁵¹M. Daene, M. Lueders, A. Ernst, D. Ködderitzsch, W. M. Temmerman, Z. Szotek and W. Hergert, *J. Phys. Cond. Matter*, 2009, **21**, 045604.
- ⁵²Z. Szotek, W. Temmerman and H. Winter, *Physica B: Condensed Matter*, 1991, **172**, 19–25.
- ⁵³J. Messud, P. M. Dinh, P.-G. Reinhard and E. Suraud, *Phys. Rev. Lett.*, 2008, **101**, 096404.
- ⁵⁴J. Messud, P. M. Dinh, P.-G. Reinhard and E. Suraud, *Chem. Phys. Lett.*, 2008, **461**, 316–320.
- ⁵⁵M. Lundberg and P. E. M. Siegbahn, *J. Chem. Phys.*, 2005, **122**, 224103.
- ⁵⁶T. Körzdörfer, M. Mundt and S. Kümmel, *Phys. Rev. Lett.*, 2008, **100**, 133004.
- ⁵⁷T. Körzdörfer, S. Kümmel and M. Mundt, *J. Chem. Phys.*, 2008, **129**, 014110.
- ⁵⁸I. Ciofini, C. Adamo and H. Chermette, *Chem. Phys.*, 2005, **309**, 67–76.
- ⁵⁹T. Baruah, R. R. Zope, A. Kshirsagar and R. K. Pathak, *Phys. Rev. A*, 1994, **50**, 2191–2196.
- ⁶⁰A. I. Johnson, K. P. K. Withanage, K. Sharkas, Y. Yamamoto, T. Baruah, R. R. Zope, J. E. Peralta and K. A. Jackson, *J. Chem. Phys.*, 2019, **151**, 174106.
- ⁶¹J. Vargas, P. Ufondu, T. Baruah, Y. Yamamoto, K. A. Jackson and R. R. Zope, *Phys. Chem. Chem. Phys.*, 2020, **22**, 3789–3799.
- ⁶²K. Trepte, S. Schwalbe, T. Hahn, J. Kortus, D.-Y. Kao, Y. Yamamoto, T. Baruah, R. R. Zope, K. P. K. Withanage, J. E. Peralta and K. A. Jackson, *J. Comput. Chem.*, 2019, **40**, 820–825.
- ⁶³K. P. K. Withanage, K. Trepte, J. E. Peralta, T. Baruah, R. Zope and K. A. Jackson, *J. Chem. Theory Comput.*, 2018, **14**, 4122–4128.
- ⁶⁴M. R. Pederson, T. Baruah, D.-y. Kao and L. Basurto, *J. Chem. Phys.*, 2016, **144**, 164117.
- ⁶⁵S. Schwalbe, L. Fiedler, T. Hahn, K. Trepte, J. Kraus and J. Kortus, *PyFLOSIC - Python based Fermi-Löwdin orbital self-interaction correction*, 2019.

- ⁶⁶D.-y. Kao, K. Withanage, T. Hahn, J. Batool, J. Kortus and K. Jackson, *J. Chem. Phys.*, 2017, **147**, 164107.
- ⁶⁷R. P. Joshi, K. Treppe, K. P. K. Withanage, K. Sharkas, Y. Yamamoto, L. Basurto, R. R. Zope, T. Baruah, K. A. Jackson and J. E. Peralta, *J. Chem. Phys.*, 2018, **149**, 164101.
- ⁶⁸K. Sharkas, L. Li, K. Treppe, K. P. K. Withanage, R. P. Joshi, R. R. Zope, T. Baruah, J. K. Johnson, K. A. Jackson and J. E. Peralta, *J. Phys. Chem. A*, 2018, **122**, 9307–9315.
- ⁶⁹K. A. Jackson, J. E. Peralta, R. P. Joshi, K. P. Withanage, K. Treppe, K. Sharkas and A. I. Johnson, *J. Phys. Conf. Ser.*, 2019, **1290**, 012002.
- ⁷⁰K. Sharkas, K. Wagle, B. Santra, S. Akter, R. R. Zope, T. Baruah, K. A. Jackson, J. P. Perdew and J. E. Peralta, *Proceedings of the National Academy of Sciences*, 2020, **117**, 11283–11288.
- ⁷¹M. R. Pederson, R. A. Heaton and C. C. Lin, *J. Chem. Phys.*, 1984, **80**, 1972–1975.
- ⁷²M. R. Pederson, R. A. Heaton and C. C. Lin, *J. Chem. Phys.*, 1985, **82**, 2688–2699.
- ⁷³W. L. Luken and D. N. Beratan, *Theor. Chem. Acc.*, 1982, **61**, 265–281.
- ⁷⁴W. L. Luken and J. C. Culberson, *Theor. Chem. Acc.*, 1984, **66**, 279–293.
- ⁷⁵M. R. Pederson, A. Ruzsinszky and J. P. Perdew, *J. Chem. Phys.*, 2014, **140**, 121103.
- ⁷⁶M. R. Pederson and T. Baruah, *Advances In Atomic, Molecular, and Optical Physics*, Academic Press, 2015, vol. 64, pp. 153–180.
- ⁷⁷R. P. Joshi, J. J. Phillips and J. E. Peralta, *Journal of Chemical Theory and Computation*, 2016, **12**, 1728–1734.
- ⁷⁸R. R. Zope, T. Baruah and K. A. Jackson, *FLOSIC 0.2*, <https://http://flosic.org/>, based on the NRLMOL code of M. R. Pederson.
- ⁷⁹K. P. K. Withanage, S. Akter, C. Shahi, R. P. Joshi, C. Diaz, Y. Yamamoto, R. Zope, T. Baruah, J. P. Perdew, J. E. Peralta and K. A. Jackson, *Phys. Rev. A*, 2019, **100**, 012505.
- ⁸⁰C. Shahi, P. Bhattarai, K. Wagle, B. Santra, S. Schwalbe, T. Hahn, J. Kortus, K. A. Jackson, J. E. Peralta, K. Treppe, S. Lehtola, N. K. Nepal, H. Myneni, B. Neupane, S. Adhikari, A. Ruzsinszky, Y. Yamamoto, T. Baruah, R. R. Zope and J. P. Perdew, *J. Chem. Phys.*, 2019, **150**, 174102.
- ⁸¹Y. Yamamoto, C. M. Diaz, L. Basurto, K. A. Jackson, T. Baruah and R. R. Zope, *J. Chem. Phys.*, 2019, **151**, 154105.
- ⁸²M. R. Pederson and T. Baruah, unpublished.

- ⁸³Y. Yamamoto, S. Romero, T. Baruah and R. R. Zope, *The Journal of Chemical Physics*, 2020, **152**, 174112.
- ⁸⁴S. Klüpfel, P. Klüpfel and H. Jónsson, *J. Chem. Phys.*, 2012, **137**, 124102.
- ⁸⁵S. Klüpfel, P. Klüpfel and H. Jónsson, *Phys. Rev. A*, 2011, **84**, 050501.
- ⁸⁶E. Ö. Jónsson, S. Lehtola and H. Jónsson, *Procedia Computer Science*, 2015, **51**, 1858–1864.
- ⁸⁷J. P. Perdew, A. Ruzsinszky, J. Sun and M. R. Pederson, *Advances In Atomic, Molecular, and Optical Physics*, Academic Press, 2015, vol. 64, pp. 1–14.
- ⁸⁸A. Ruzsinszky, J. P. Perdew, G. I. Csonka, O. A. Vydrov and G. E. Scuseria, *J. Chem. Phys.*, 2006, **125**, 194112.
- ⁸⁹J. Jaramillo, G. E. Scuseria and M. Ernzerhof, *J. Chem. Phys.*, 2003, **118**, 1068–1073.
- ⁹⁰T. Schmidt, E. Kraisler, A. Makmal, L. Kronik and S. Kummel, *The Journal of Chemical Physics*, 2014, **140**, 18A510.
- ⁹¹J. C. Slater and J. H. Wood, *International Journal of Quantum Chemistry*, 1970, **5**, 3–34.
- ⁹²R. A. Heaton, J. G. Harrison and C. C. Lin, *Phys. Rev. B*, 1983, **28**, 5992–6007.
- ⁹³J. G. Harrison, R. A. Heaton and C. C. Lin, *Journal of Physics B: Atomic and Molecular Physics*, 1983, **16**, 2079–2091.
- ⁹⁴Y. Yamamoto, L. Basurto, C. M. Diaz, R. R. Zope and T. Baruah, *Self-interaction correction to density functional approximations using Fermi-Löwdin orbitals: methodology and parallelization*, Unpublished.
- ⁹⁵D. Porezag and M. R. Pederson, *Phys. Rev. A*, 1999, **60**, 2840–2847.
- ⁹⁶M. R. Pederson and K. A. Jackson, *Phys. Rev. B*, 1990, **41**, 7453–7461.
- ⁹⁷P. Bhattarai, K. Wagle, C. Shahi, Y. Yamamoto, S. Romero, B. Santra, R. R. Zope, J. E. Peralta, K. A. Jackson and J. P. Perdew, *The Journal of Chemical Physics*, 2020, **152**, 214109.
- ⁹⁸S. J. Chakravorty, S. R. Gwaltney, E. R. Davidson, F. A. Parpia and C. F. Fischer, *Phys. Rev. A*, 1993, **47**, 3649–3670.
- ⁹⁹A. Kramida, Yu. Ralchenko, J. Reader and NIST ASD Team, NIST Atomic Spectra Database (ver. 5.6.1), [Online]. Available: <https://physics.nist.gov/asd> [2018, July 25]. National Institute of Standards and Technology, Gaithersburg, MD., 2018.
- ¹⁰⁰National Institute of Standards and Technology, NIST Computational Chemistry Comparison and Benchmark Database NIST Standard Reference Database Number 101

Release 19, April 2018, Editor: Russell D. Johnson III <http://cccbdb.nist.gov/>
DOI:10.18434/T47C7Z.

- ¹⁰¹L. A. Curtiss, K. Raghavachari, G. W. Trucks and J. A. Pople, *J. Chem. Phys.*, 1991, **94**, 7221–7230.
- ¹⁰²B. J. Lynch and D. G. Truhlar, *J. Phys. Chem. A*, 2003, **107**, 8996–8999.
- ¹⁰³R. Peverati and D. G. Truhlar, *J. Chem. Phys.*, 2011, **135**, 191102.
- ¹⁰⁴J. Zheng, Y. Zhao and D. G. Truhlar, *J. Chem. Theory Comput.*, 2007, **3**, 569–582.
- ¹⁰⁵L. Goerigk, A. Hansen, C. Bauer, S. Ehrlich, A. Najibi and S. Grimme, *Phys. Chem. Chem. Phys.*, 2017, **19**, 32184–32215.
- ¹⁰⁶L. Goerigk and S. Grimme, *J. Chem. Theory Comput.*, 2010, **6**, 107–126.
- ¹⁰⁷A. Ruzsinszky, J. P. Perdew and G. I. Csonka, *The Journal of Physical Chemistry A*, 2005, **109**, 11006–11014.
- ¹⁰⁸S. Akter, Y. Yamamoto, C. M. Diaz, K. A. Jackson, R. R. Zope and T. Baruah.
- ¹⁰⁹V. S. Bryantsev, M. S. Diallo, A. C. T. van Duin and W. A. Goddard, *Journal of Chemical Theory and Computation*, 2009, **5**, 1016–1026.
- ¹¹⁰D. Manna, M. K. Kesharwani, N. Sylvetsky and J. M. L. Martin, *J. Chem. Theory Comput.*, 2017, **13**, 3136–3152.
- ¹¹¹B. Santra and J. P. Perdew, *J. Chem. Phys.*, 2019, **150**, 174106.
- ¹¹²J. W. Furness and J. Sun, *Phys. Rev. B*, 2019, **99**, 041119.

This figure "he_hep.jpg" is available in "jpg" format from:

<http://arxiv.org/ps/2010.08921v1>